

Electron doped $\text{Sr}_2\text{IrO}_{4-\delta}$ ($0 \leq \delta \leq 0.04$): Evolution of a disordered $J_{\text{eff}} = 1/2$ Mott insulator into an exotic metallic state

Cite as: J. Appl. Phys. **109**, 07D906 (2011); <https://doi.org/10.1063/1.3545803>

Submitted: 24 September 2010 • Accepted: 08 November 2010 • Published Online: 22 March 2011

T. F. Qi, O. B. Korneta, S. Chikara, et al.



View Online



Export Citation

ARTICLES YOU MAY BE INTERESTED IN

[Tuning electronic structure via epitaxial strain in \$\text{Sr}_2\text{IrO}_4\$ thin films](#)

Applied Physics Letters **102**, 141908 (2013); <https://doi.org/10.1063/1.4801877>

[Structure, magnetism, and transport properties for Ca doping in \$\text{Sr}_2\text{IrO}_4\$](#)

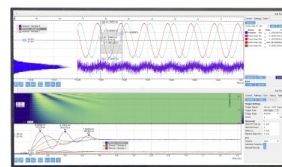
AIP Advances **7**, 055823 (2017); <https://doi.org/10.1063/1.4976736>

[\$\text{Sr}_2\text{IrO}_4\$: Gateway to cuprate superconductivity?](#)

APL Materials **3**, 062404 (2015); <https://doi.org/10.1063/1.4921953>

Challenge us.

What are your needs for
periodic signal detection?



Zurich
Instruments



Electron doped $\text{Sr}_2\text{IrO}_{4-\delta}$ ($0 \leq \delta \leq 0.04$): Evolution of a disordered $J_{\text{eff}} = 1/2$ Mott insulator into an exotic metallic state

T. F. Qi^{1,2} O. B. Korneta^{1,2} S. Chikara^{1,2} M. Ge^{1,5} S. Parkin^{1,3} L. E. De Long^{1,2}
P. Schlottmann, and G. Cao^{1,2,a)}

¹Center for Advanced Materials, University of Kentucky, Lexington, Kentucky 40506, USA

²Department of Physics and Astronomy, University of Kentucky, Lexington, Kentucky 40506, USA

³Department of Chemistry, University of Kentucky, Lexington, Kentucky 40506, USA

⁴Department of Physics, Florida State University, Florida 32306, USA

⁵University of Science and Technology of China, Hefei 230026, China

(Presented 15 November 2010; received 24 September 2010; accepted 8 November 2010; published online 22 March 2011)

Stoichiometric Sr_2IrO_4 is a ferromagnetic $J_{\text{eff}} = [1/2]$ Mott insulator driven by strong spin-orbit coupling. Introduction of very dilute oxygen vacancies into single-crystal $\text{Sr}_2\text{IrO}_{4-\delta}$ with $\delta \leq 0.04$ leads to significant changes in lattice parameters and an insulator-to-metal transition at $T_{\text{MI}} = 105$ K. The highly anisotropic electrical resistivity of the low-temperature metallic state for $\delta \approx 0.04$ exhibits anomalous properties characterized by non-Ohmic behavior and an abrupt current-induced transition in the resistivity at $T^* = 52$ K, which separates two regimes of resistive switching in the nonlinear I-V characteristics. The novel behavior illustrates an exotic ground state and constitutes a new paradigm for devices structures in which electrical resistivity is manipulated via low-level current densities ~ 10 mA/cm² (compared to higher spin-torque currents $\sim 10^7$ – 10^8 A/cm²) or magnetic inductions ~ 0.1 – 1.0 T. © 2011 American Institute of Physics. [doi:10.1063/1.3545803]

It is commonly expected that iridates are more metallic and less magnetic than their 3d and 4d counterparts. The extended nature of 5d orbitals leads to a broad 5d bandwidth and a reduced Coulomb interaction U , such that the Stoner criterion anticipates a metallic, paramagnetic state. In marked contrast, many iridates are magnetic insulators (e.g., BaIrO_3 , Sr_2IrO_4 , and $\text{Sr}_3\text{Ir}_2\text{O}_7$), while the correlated metal SrIrO_3 is an exception.^{1–12} The unusual properties of Sr_2IrO_4 have been attributed to the interplay of a strong spin-orbit interaction with a comparable crystalline electric field splitting,^{2–5} which leads to a novel $J_{\text{eff}} = 1/2$ Mott state^{6,7} associated with a topological phase.⁹ Sr_2IrO_4 is a weak ferromagnet (FM) ($T_{\text{C}} = 240$ K) with a saturation moment of no greater than $0.14 \mu_{\text{B}}/\text{Ir}$.^{5,8} The competition between magnetic exchange interactions and lattice distortions in Sr_2IrO_4 gives rise to a giant magnetodielectric shift (of order 100% in magnetic inductions $B \leq 1$ T) that is driven by spin-orbit coupling rather than magnetization.⁸

Here, we report that the introduction of very dilute oxygen vacancies into single-crystal $\text{Sr}_2\text{IrO}_{4-\delta}$ drives the following intriguing phenomena: (1) An insulator-to-metal transition signaled by a highly anisotropic resistivity that continues to decrease by several orders of magnitude below a temperature $T_{\text{MI}} (\geq 105$ K for $\delta \leq 0.04$), without saturation to a residual limit at the lowest temperature studied ($T = 1.8$ K). (2) Non-linear I-V behavior occurs with switching at three modest current thresholds (~ 10 A. cm⁻²). (3) An abrupt current-induced transition in the resistivity at $T^* = 52$ K separates two temperature regimes with different nonlinear I-V characteristics.

Synthesis of flux-grown single-crystal Sr_2IrO_4 is described elsewhere.^{5,8,11,12} The crystal structures of both stoichiometric

Sr_2IrO_4 and nonstoichiometric $\text{Sr}_2\text{IrO}_{4-\delta}$ ($\delta \leq 0.04$) single crystals were determined at $T = 90$ K and 295 K using a Nonius Kappa CCD x-Ray diffractometer and Mo $K\alpha$ radiation. Chemical compositions of the single crystals were determined using energy dispersive x-ray analysis. Unlike cuprate single crystals that require a complex post-annealing sequence and a long diffusion time (e.g., days or even weeks) to significantly alter physical properties, single-crystal samples of the layered iridates undergo significant structural alterations and radical changes in bulk transport and magnetic properties after merely hours of post annealing. Reduced oxygen content ($0 \leq \delta \leq 0.04$) was generated by firing an as-grown single-crystal Sr_2IrO_4 in a TGA (Mettler-Toledo Model TGA/DSC 1) or an evacuated quartz tube at 600 °C for different periods of time, depending on the composition $\text{Sr}_2\text{IrO}_{4-\delta}$ sought. (We note that structural and physical properties of other iridates such as $\text{Sr}_3\text{Ir}_2\text{O}_7$ and BaIrO_3 show the same sensitivity to oxygen depletion.) Values of δ were determined in the TGA measurements. I-V characteristics were obtained using a Keithley 6220 current source and a Keithley 2182A nanovoltmeter. The differential resistance was measured using a built-in function of the above Keithley meters to eliminate potential thermoelectric voltages on the contact leads. Comparisons between the differential resistance and conventional resistance revealed no differences whatsoever, indicating contact effects were negligible. Measurements of magnetization $M(T,H)$, electrical resistivity $\rho(T,H)$, and thermopower $S(T)$ were performed using either a Quantum Design physical property measurement system (PPMS) or magnetic Property Measurement System (MPMS), as described elsewhere.⁸

Sr_2IrO_4 crystallizes in a reduced tetragonal structure (space-group $I4_1/acd$) due to a rotation of the IrO_6 -octahedra about the c -axis by an angle $\sim 11^\circ$.^{2–4} This rotation corresponds to a distorted in-plane Ir1-O2-Ir1 bond angle θ that

a) Author to whom correspondence should be addressed: 177 Chemistry-Physics Building, University of Kentucky, Lexington, KY 40506. Electronic mail: cao@pa.uky.edu.

decreases with decreasing temperature. Our single-crystal x-ray diffraction data confirm this trend for stoichiometric crystals ($\delta = 0$), and also reveal that θ for $\delta = 0.04$ increases slightly with decreasing temperature from 157.028° at 295 K to 157.072° at 90 K, and the latter angle is significantly larger than that for $\delta = 0$, (i.e., $\theta = 156.280^\circ$ at 90 K), as shown in Table I. The increment $D_q = 0.792^\circ$ is large for such a small oxygen depletion. Moreover, the volume of the unit cell V for $\delta \approx 0.04$ contracts by an astonishing 0.14% compared to that for $\delta = 0$ (see Table I). These data indicate that dilute oxygen vacancies relax θ and reverse its temperature dependence with increasing δ , while significantly reducing the structural distortion at low T . No such changes in the lattice parameters would be observable in x-ray diffraction data should the oxygen depletion be confined to the crystal surface and not uniformly distributed within the bulk.

The Ir1-O2-Ir1 bond angle θ is an important focus of this study, as it controls the hopping of the 5d electrons and super-exchange interactions between Ir atoms via the bridging O sites,¹⁰ and is therefore expected to influence physical properties. For example, the **a**-axis resistivity ρ_a (**c**-axis resistivity ρ_c) is reduced by a factor of 10^{-9} (10^{-7}) with doping at $T = 1.8$ K as δ changes from 0 to ~ 0.04 [see Fig. 1(a) and 1(b)]. For $\delta \approx 0.04$, there is a sharp insulator-to-metal transition near $T_{MI} = 105$ K, resulting in a reduction of ρ_a (ρ_c) by a factor of 10^{-4} (10^{-1}), from just below T_{MI} to $T = 1.8$ K [Fig. 1(b)]. The strong low- T anisotropy reflected in the values of ρ_a and ρ_c and their sensitivity to δ are consistent with a nearly 2D, strongly correlated electron system. Below 20 K, ρ_a has linear- T dependence without saturation to a residual resistivity limit; and although there is a plateau in ρ_c for $5 < T < 35$ K, it is followed by a very rapid downturn near $T_a = 5$ K [Fig. 1(b), inset], which indicates a sudden, rapid decrease in inelastic scattering.

Oxygen depletion also changes the electronic density of states $g(E_F)$ of $\text{Sr}_2\text{IrO}_{4-\delta}$, as reflected in the thermoelectric power $S(T)$, as shown in Fig. 1(c). A peak in the **c**-axis $S_c(T)$ for $\delta = 0.04$ is only $\sim 1/3$ of the peak value observed for $\delta = 0$. Since $S(T)$ measures the voltage induced by a temperature gradient (which cannot be confined to the surface of the crystal), the drastic changes in $S(T)$ shown in Fig. 1(c) further reinforces our conclusion that oxygen depletion is a bulk effect, as indicated by the observed changes in lattice parameters discussed above. The strong reduction of $S_c(T)$ for $\delta \approx 0.04$ indicates an increase of $g(E_F)$ with increasing δ , since $S \propto 1/g(E_F)$.¹³ The rapid increase of $g(E_F)$ with increasing δ is also evident in the decrease of the **a**-axis resistivity ($T = 1.8$ K) by nine orders of magnitude as δ changes from 0 to ~ 0.04 . These rapid changes in transport properties with doping are much stronger than those observed for Lifshitz transitions in metallic alloys where the Fermi level crosses small pockets with doping or applied pressure.¹⁴ On the other hand,

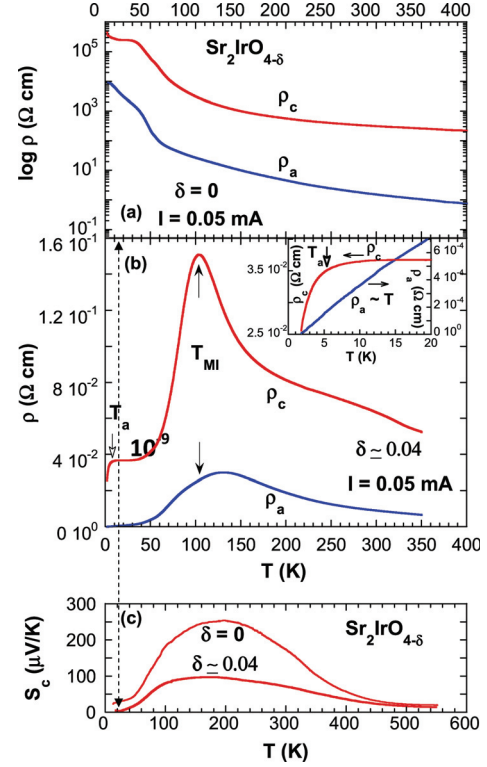


FIG. 1. (Color online) The **a**- and **c**-axis resistivity ρ_a and ρ_c as a function of temperature for (a) $\delta = 0$ and (b) $\delta \approx 0.04$; (c) **c**-axis thermoelectric power $S_c(T)$ for $\delta = 0$ and $\delta \approx 0.04$. Inset in (b): ρ_a and ρ_c vs T for $1.7 \text{ K} < T \leq 20 \text{ K}$; note a downturn near 5 K in ρ_c and linear temperature dependence in ρ_a .

they are reminiscent of the extreme sensitivity of “correlation-gap insulators” to dilute impurities and pressure.^{15,16}

Strong crystal fields split off 5d-band states with e_g symmetry in stoichiometric Sr_2IrO_4 , and t_{2g} bands arise from $J = 1/2$ and $J = 3/2$ multiplets via strong spin-orbit coupling. A weak admixture of the e_g orbitals downshifts the $J = 3/2$ quadruplet from the $J = 1/2$ doublet.^{6,7} An independent electron picture anticipates a metallic state, since the Ir^{4+} ($5d^5$) ions provide four electrons to fill the lower $J_{\text{eff}} = 3/2$ bands, plus one electron to partially fill the $J_{\text{eff}} = 1/2$ bands. However, the $J_{\text{eff}} = 1/2$ bandwidth W ($W = 0.48 \text{ eV}$ for $\delta = 0$) is so narrow, even a modest U ($\sim 0.5 \text{ eV}$) is sufficient to induce a Mott gap $\Delta \sim 0.5 \text{ eV}$ in the $J_{\text{eff}} = 1/2$ band.⁶ W is quite sensitive to structural alterations according to a recent first-principles calculation¹⁰ that predicts that an increased θ should cause a broadening of the $J_{\text{eff}} = 1/2$ band and a concomitant decrease of the Mott gap by 0.13 eV , if θ increases from 157° to 170° . The observed increment $\Delta\theta = 0.792^\circ$ does not appear nearly sufficient to produce the dramatic changes we have observed in ρ , and we conclude that another mechanism must be responsible for T_{MI} .

Removal of oxygen from $\text{Sr}_2\text{IrO}_{4-\delta}$ is expected to result in electron doping of the insulating state that is observed to be stable for $\delta = 0$. According to (LDA+SO+U) band structure calculations¹⁰ additional electrons will occupy states in four symmetric pockets located near the M-points of the basal plane of the Brillouin zone. Each pocket has an estimated filling of 2% of the Brillouin zone for $\delta = 0.04$. The situation appears analogous to doping in strongly correlated $(\text{La}_{1-x}\text{Sr}_x)_2\text{CuO}_4$ (LSCO) (where pockets of similar shape arise at the

TABLE I. Lattice parameters at $T = 90 \text{ K}$ for $\delta = 0$ and 0.04.

δ ($T = 90 \text{ K}$)	a (\AA)	c (\AA)	V (\AA^3)	Ir1-O2-Ir1 bond angle θ
0	5.4836(8)	25.8270(5)	776.61(22)	156.280°
0.04	5.4812(3)	25.8146(16)	775.56(8)	157.072°

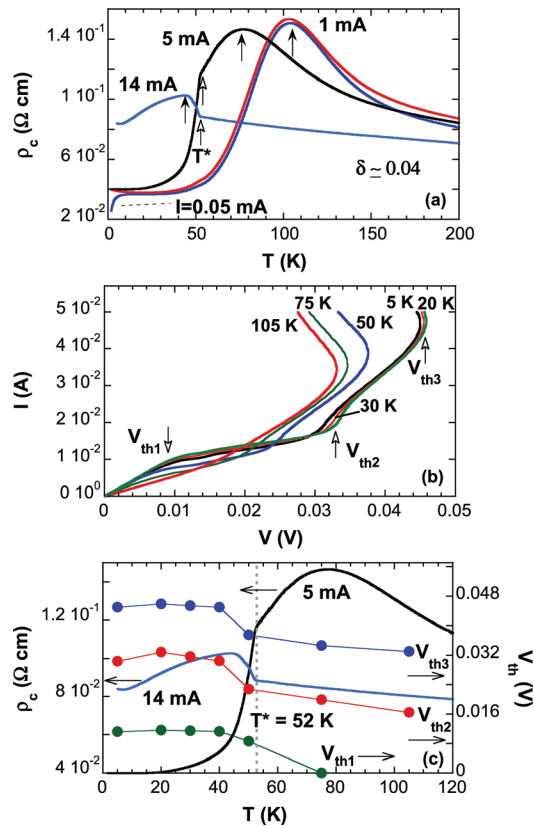


FIG. 2. (Color online) (a) Temperature dependence of ρ_c for several representative values of current I ; (b) I - V curves at several representative temperatures and (c) temperature dependence of ρ_c at $I=5$ and 14 mA and threshold V_{th} (right scale).

same positions in the Brillouin zone) and $\text{La}_2\text{CuO}_{4+\delta}$.¹⁷ There are, however, two fundamental differences: While in $\text{Sr}_2\text{IrO}_{4-\delta}$ we dope electrons, the added carriers are holes in the cuprates; moreover, Sr_2IrO_4 is a weak ferromagnet rather than a simple antiferromagnet, as is La_2CuO_4 .

Oxygen depletion also introduces disorder, which is expected to lead to localization of states close to the band-edge in a quasi-2D system.¹⁸ We assume that the Fermi level lies below the mobility edge for $\delta \neq 0$, and hence, the occupied states are all localized at high T , where the compound is a paramagnetic insulator. As T is lowered, the compound develops increasing FM polarization below T_C and the intersection of the Fermi level with the majority spin band is gradually pushed closer to the mobility edge as the exchange splitting of the band increases below T_C . Eventually the Fermi level crosses the mobility edge, leading to metallic behavior below T_{MI} .

The exotic nature of the metallic state of $\text{Sr}_2\text{IrO}_{4-\delta}$ is revealed in striking non-Ohmic behavior, as exhibited by $\rho_c(T)$ for various applied currents I [see Fig. 2(a)]; ρ_a behaves similarly, and is not shown). ρ_c changes slightly when $I \leq 1$ mA, but more dramatically when $I \geq 5$ mA (~ 10 A/cm² current density). Moreover, there is a characteristic temperature $T^* = 52$ K at which ρ_c sharply drops for $I = 5$ mA, but rises for $I = 14$ mA [see Figs. 2(a) and 2(c)], indicating a current-induced phase transition. Interestingly, the distinct downturn in ρ_c below $T_a \approx 5$ K disappears for $I \geq 1$ mA.

The nonlinear I - V characteristic shown in Fig. 2(b) shows switching occurs at multiple threshold potentials as I varies

from $0.1 \mu\text{A}$ to 50 mA. We infer a temperature T^* that separates two different regions: For $T < T^*$, there are three threshold potentials V_{th1} , V_{th2} , and V_{th3} . The initial linearity in the I - V curve persists up to $I = 4$ mA for $V < V_{th1}$ ($= 0.011$ V at 5 K); between V_{th1} and V_{th2} linearity is briefly restored with a reduced slope. With further increases in I , the I - V response exhibits a third threshold V_{th3} , which marks the onset of current-controlled negative differential resistivity (NDR), where V across the crystal decreases as I increases. The qualitative difference between the two regions separated by T^* is clearly revealed in the temperature dependences of V_{th1} , V_{th2} , and V_{th3} , as well as ρ_c , at $I = 5$ and 14 mA, as shown in Fig. 2(c). Note that V_{th2} and V_{th3} increase with increasing T below T^* . For $T > T^*$, the trend is reversed: V_{th3} and V_{th2} shift to lower values, and V_{th1} tends to zero with increasing T . Note that T^* remains sharply defined in $\rho_c(T)$ at 52 K, independent of I [Fig. 2(c)]. This completely rules out the possibility that self-heating plays a role in the non-Ohmic behavior.

The observed non-Ohmic behavior of the metallic state therefore poses intriguing questions concerning its origin: Does non-Ohmic behavior observed in both the insulating and metallic states of iridates arise from the same mechanism—i.e., a CDW state? Note that the voltage thresholds ($\sim 10^{-2}$ V) observed for $\delta = 0.04$ are two orders of magnitude smaller than those (~ 1 V) observed in CDW depinning experiments,¹⁹ which would suggest an extremely weak CDW pinning by defects that has not been reported before. Otherwise, the observed non-Ohmic behavior of the metallic state must signal a metallic state that does not follow Ohm's law.

The behavior of $\text{Sr}_2\text{IrO}_{4-\delta}$ clearly illustrates an intrinsically unstable ground state that readily swings between highly insulating ($10^5 \Omega \text{ cm}$) and metallic ($10^{-5} \Omega \text{ cm}$) states via only very slight changes in oxygen content. The non-Ohmic behavior, whose origin is yet to be fully understood, constitutes a paradigm for device structures in which resistivity can be manipulated with modest applied currents rather than large magnetic fields or much larger voltages.

G. C. is thankful to Dr. M. Whangbo and Dr. J. W. Brill for useful discussions. This work was supported by the NSF through Grants Nos. DMR-0552267, DMR-0856234, and EPS-0814194 (G.C.), and by DOE through Grants Nos. DE-FG02-97ER45653 (L.E.D.) and DE-FG02-98ER45707 (P.S.).

¹G. Cao *et al.* *Solid State Commun.* **113**, 657 (2000).

²M.K. Crawford *et al.* *J. Phys. Rev. B* **49**, 9198 (1994).

³Q. Huang *et al.* *Solid State Chem.* **112**, 355 (1994).

⁴R. J. Cava *et al.* *Phys. Rev. B* **49**, 11890 (1994).

⁵G. Cao *et al.* *Phys. Rev. B* **57**, R11039 (1998).

⁶B. J. Kim *et al.* *Phys. Rev. Lett.* **101**, 076402 (2008).

⁷S. J. Moon *et al.* *Phys. Rev. Lett.* **101**, 226402 (2008).

⁸S. Chikara *et al.* *Phys. Rev. B* **80**, 140407(R) (2009).

⁹B. J. Kim *et al.* *Science* **323**, 1329 (2009).

¹⁰S. J. Moon *et al.* *Phys. Rev. B* **80**, 195110 (2009).

¹¹G. Cao *et al.* *Phys. Rev. B* **66**, 214412 (2002).

¹²G. Cao *et al.* *Phys. Rev. B* **76**, 100402(R) (2007).

¹³P. A. Cox, *Transition Metal Oxides* (Clarendon Press, Oxford, 1995), p. 163.

¹⁴T. F. Smith, *J. Low Temp. Phys.* **11**, 581 (1973).

¹⁵P. Schlottmann, *Phys. Rev. B* **46**, 998 (1992).

¹⁶J. Beille *et al.* *Phys. Rev. B* **28**, 7397 (1983).

¹⁷J. D. Jorgensen *et al.* *Phys. Rev. B* **38**, 11337 (1988).

¹⁸N. F. Mott, *Metal-Insulator Transitions* (Taylor and Francis, London, 1990), p. 36.

¹⁹G. Gruner, *Density Waves in Solids* (Addison-Wesley, New York, 1994).